BRITISH ECOLOGICAL SOCIETY Functional Ecology

The negative effects of an allelopathic invader on native plant photosynthesis are amplified after tree canopy closure

Journal:	*Functional Ecology*
Manuscript ID	FE-2025-01432.R1
Wiley - Manuscript type:	Research Article
Key-words:	Alliaria petiolata, AM fungi, plant invasion, stomatal conductance, J_{max}, V_{max}, symbiosis

"The negative effects of an allelopathic invader on native plant photosynthesis are amplified after tree canopy closure"

Abstract

1. Many invasive plants produce antimicrobial allelopathic compounds that disrupt plant-fungal symbioses of native species in the communities they invade, influencing nutrient and water provisioning that support photosynthesis. Previous studies have linked these disruptions to reductions in photosynthesis and stomatal conductance, but whether these effects are tied to reductions in photosynthetic capacity remains unclear, limiting inferences about the mechanisms driving physiological responses of native species. Furthermore, how these responses vary temporally across the growing season is unknown.
2. To investigate the temporal dynamics of native plant responses to allelopathic invasion, we measured gas exchange in two understory native species (*Trillium* spp. and *Maianthemum racemosum*) at two points during the growing season – before and after tree canopy closure. Plants were measured in a long-term field experiment where *Alliaria petiolata*, an allelopathic invader known to disrupt AM fungal symbioses, has been removed or left at ambient levels since 2006.
3. Both native species exhibited significantly reduced net photosynthesis rates under ambient *A. petiolata* levels compared to the weeded treatment. This response was due to a reduction in apparent photosynthetic capacity in *Trillium* spp. and a reduction in stomatal conductance that increased stomatal limitation in *M. racemosum*. Photosynthetic responses to *A. petiolata* in both species were amplified after tree canopy closure.
4. *Alliaria petiolata* reduced native plant net photosynthesis either by increasing nutrient stress, as indicated by the reduction in apparent photosynthetic capacity (*Trillium* spp.), or by increasing water stress, as indicated by the reduction in stomatal conductance (*M. racemosum*), and that these responses only amplified after the tree canopy closed. These results highlight the importance of seasonal changes that can regulate plant physiological responses to allelopathic invaders and demonstrate the diversity of mechanisms by which allelopathic invaders can influence native plant physiology.

Keywords
Alliaria petiolata, AM fungi, photosynthesis, plant invasion, symbiosis, stomatal conductance, V_{cmax}, J_{max}

Introduction

Invasive plants often express unique traits that increase their likelihood of establishment in novel ecosystems. Allelopathy, defined as a secondary compound produced by a plant that negatively impacts neighboring plant species and/or soil microbial communities (Inderjit et al., 2011), has emerged as a mechanism to explain the success of some invasive plant species (Callaway et al., 2008; Callaway & Ridenour, 2004). Allelopathy occurs in ~52% of invasive plant species (Kalisz et al., 2021) and negatively affects native plant performance and soil microbial community composition in both field and greenhouse settings (Bialic-Murphy et al., 2020, 2021; Brouwer et al., 2015; Hale et al., 2011, 2016; Hale & Kalisz, 2012; Qu et al., 2021; Roche et al., 2021; Zhang et al., 2021). Despite the prevalence of allelopathy among invasive species, we do not fully understand the mechanisms that drive native plant physiological responses to allelopathic invasion or the temporal dynamics that underpin these responses. This knowledge gap hinders our understanding of how the disruptive impacts of allelopathic invasion on soil microbial communities scale to influence plant community dynamics.

Photosynthesis links ecosystem carbon, nutrient, and water cycles in terrestrial ecosystems (Hungate et al., 2003). Photosynthetic enzymes, such as Ribulose-1,5-bisphosphate (RuBP) carboxylase/oxygenase (Rubisco), require substantial nutrients and energy for their construction and maintenance, creating a large nutrient and energy demand for the plant (Evans & Clarke, 2019; Evans & Seemann, 1989). Photosynthetic capacity, or the biochemical capacity at which a leaf can fix carbon, can be estimated from the maximum rate of Rubisco carboxylation (V_{cmax}) and the maximum rate of electron transport for RuBP regeneration (J_{max}) (Ali et al., 2015; Farquhar et al., 1980). These gas exchange-derived parameters are often standardized to a common temperature to remove the influence of enzyme kinetics and make inferences about biochemical investment in photosynthesis (Way & Yamori, 2014). This standardization is commonly done at 25°C, represented as V_{cmax25} and J_{max25} from this point forward. V_{cmax25} and J_{max25} are often positively correlated with leaf nitrogen and phosphorus content and are commonly used as indicators of nutrient stress (Ellsworth et al., 2022; Evans,

1989; Walker et al., 2014). Photosynthesis is also regulated by stomatal conductance, which controls CO_2 diffusion into leaves and supports transpiration (Farquhar & Sharkey, 1982). Transpiration allows for the uptake and transport of water and nutrients by the roots through the plant vascular system to photosynthetic tissues. Stomata close and stomatal conductance generally declines with increasing water limitation, making it a useful indicator of water stress (Medrano et al., 2002). Because leaf-level photosynthesis reflects photosynthetic capacity and stomatal conductance, assessing how both respond individually to allelopathic invaders can clarify the physiological mechanisms that drive native species responses.

Allelopathic compounds with antimicrobial properties can inhibit the growth and reproduction of soil microbial communities, such as mycorrhizal fungi, which are essential for plant nutrient and water uptake (Hale & Kalisz, 2012). Arbuscular mycorrhizal (AM) fungi often form obligate symbioses with plants, exchanging mineral nutrients and water for photosynthate (S. E. Smith & Read, 2008). Antimicrobial compounds produced by allelopathic invaders can inhibit AM fungal spore germination, fungal root colonization, and arbuscule formation, which can decrease AM fungal biomass in roots and soil, alter AM fungal species richness, and modify AM fungal community composition (Burke, 2008; Callaway et al., 2008; Burke et al., 2011; Cantor et al., 2011; Anthony et al., 2019; Bialic-Murphy et al., 2021). These disruptions may decrease nutrient and water uptake in plants that rely on AM fungi, even when allelopathic invaders do not directly modify soil nutrient or water availability (Bialic-Murphy et al., 2021). AM fungal mutualism disruption may increase the plant carbon cost for acquiring nutrients and water, causing plants to receive less resources provisioned by AM fungal partners for a given belowground carbon investment (Hale et al., 2016; Kummel & Salant, 2006). This pattern may alter resource allocation to photosynthetic enzymes, as emerging evidence suggests that increased costs of nutrient acquisition are associated with altered nutrient allocation to photosynthetic enzymes (Perkowski et al., 2021, 2025; Waring et al., 2023). Thus, all else being equal (e.g., competition for soil resources), AM fungal mutualism disruption could cause native plants to be unable to satisfy demand to build and maintain photosynthetic enzymes and/or maintain stomatal conductance, which may explain why native species exhibit reduced net photosynthesis rates in response to allelopathic invaders (Bialic-Murphy et al., 2020; Hale et al., 2011, 2016).

Alliaria petiolata (M. Bieb) Cavara & Grande (Family: Brassicaceae) is a model species for investigating the impacts of allelopathic plant invasion on native plant communities. This biennial herb from Eurasia invades temperate forest understories in North America and releases glucosinolates into soil environments through root exudation and leaf litter (Rodgers et al., 2008). Glucosinolates produced by *A. petiolata* hydrolyze into antimicrobial compounds that inhibit AM spore germination, spore viability, root colonization, and arbuscule formation (Anthony et al., 2019; Callaway et al., 2008; Cantor et al., 2011). Field studies show that *A. petiolata* reduces AM fungal biomass, increases AM species richness, and alters fungal community composition (Table 1; Bialic-Murphy et al., 2021; Burke, 2008; Burke et al., 2011; Cantor et al., 2011). These AM fungal community disruptions negatively affect native plant nutrient and water economics, population dynamics, and community composition (Bialic-Murphy et al., 2020, 2021; Hale et al., 2016; Roche et al., 2021, 2023), with stronger impacts in AM-associating native plant species compared non-mycorrhizal species (Callaway et al., 2008; Roche et al., 2021, 2023). These patterns occur despite evidence that *A. petiolata* invasions do not affect soil nutrient or water availability, suggesting that AM fungal mutualism disruption is the likely mechanism that drives native plant responses this allelopathic invader (Bialic-Murphy et al., 2021; Burke et al., 2019).

Previous work indicates that *A. petiolata* reduces net photosynthesis and stomatal conductance in a common forest understory native species, *M. racemosum* (Brouwer et al., 2015; Hale et al., 2011, 2016). However, the mechanisms that regulate native plant responses to *A. petiolata* are not fully understood, in part because the effects of *A. petiolata* on apparent photosynthetic capacity (i.e., V_{cmax25}, J_{max25}) have not been quantified. Understanding whether changes in net photosynthesis are driven by changes in photosynthetic capacity or stomatal conductance would clarify the mechanism underlying *A. petiolata* impacts on native plant physiology. Moreover, field studies have quantified photosynthetic responses to *A. petiolata* at a single point in the growing season despite strong seasonal shifts in understory light and soil resource availability that could modulate reliance on disrupted AM fungal communities. Gas exchange measurements collected at different time points in the growing season are needed to assess the relative magnitude of leaf-level physiological responses to *A. petiolata* and how this relates to fine-scale impacts on AM fungal community composition and broad-scale effects on native plant productivity and survivorship.

Here, we assessed the temporal dynamics that drive the effects of *A. petiolata* on leaf-level photosynthetic processes of two coexisting native plant species. We collected gas exchange measurements at two timepoints (open canopy early in growing season, closed canopy later in the growing season) from two understory native species (*Trillium* spp. and *Maianthemum racemosum*) in a long-term *A. petiolata* field manipulation experiment. We used these measurements and experimental setup to test the following hypotheses:

1) Both native species will experience reduced net photosynthesis in the *A. petiolata*-ambient treatment compared to the *A. petiolata*-weeded treatment. These patterns will be associated with reduced temperature-standardized apparent photosynthetic capacity (i.e., V_{cmax25}, J_{max25}), relative chlorophyll content, and stomatal conductance, in the *A. petiolata*-ambient treatment. We expected that a reduction in apparent photosynthetic capacity and/or relative chlorophyll content in response to *A. petiolata* presence would indicate nutrient stress, while a reduction in stomatal conductance would indicate water stress.
2) The negative effects of *A. petiolata* on the photosynthetic traits of native species will depend on time in the growing season.
    a) The negative effects of *A. petiolata* on leaf photosynthetic traits will be greatest early in the growing season when photosynthetic demand is highest (due to increased understory light availability). Disrupted AM fungal symbioses will create resource stress, making it more difficult for AM-associating plants to acquire nutrients and water to satisfy photosynthetic demand.
    b) Alternatively, the negative effects of *A. petiolata* on photosynthetic traits will be greatest later in the growing season. This response may be driven by increased reliance on disrupted AM fungal partners for soil nutrients and water as resources are depleted. However, as tree canopy closure reduces light availability, photosynthetic demand may also decline, which may mitigate the effects of AM fungal mutualism disruption on late-season physiology

Materials and Methods

Study site and experimental design

This study was conducted at Trillium Trail Nature Reserve in Fox Chapel, Pennsylvania, USA (40.520 °N, -79.901 °W). The mean annual precipitation of the study area is 1006 mm yr^{-1} and the mean annual temperature is 11°C (2006-2020 U.S. Climate Normals; Palecki et al., 2021). Wire fences (2.5 m tall) were set up in 2002 at five 14 x 14 m experimental plots to exclude deer while allowing free movement of small mammals and birds. *Alliaria petiolata* has been weeded by hand at the beginning of each growth season from one half of each experimental plot since 2006, with *A. petiolata* remaining at natural densities in the other half of each plot. Weeding by hand has been an effective strategy for *A. petiolata* removal, with relative abundance of *A. petiolata* averaging 0.08% in years that followed the initial weeding treatment in 2006 with minimal disturbance to the plots (Roche et al., 2021). This long-term split-plot experiment is located on 25-75% grade slopes. Soils were classified as Gilpin-Upshur-Atkins soils with dominant shale, sandstone, and red clay shale bedrock components. *Alliaria petiolata* treatments were set up parallel to the slope to prevent allelochemical leaching into the weeded side of the plot. Previous work conducted in this experiment has shown that *A. petiolata*-ambient plots exhibit decreased AM fungal biomass, decreased AM root colonization rates, and increased AM fungal richness compared to *A. petiolata*-weeded plots (Burke, 2008; Burke et al., 2011; Cantor et al., 2011), which has altered the AM fungal community composition between treatments (Bialic-Murphy et al., 2021) (Table 1). Additionally, soil nutrient availability and soil water availability did not differ between *A. petiolata* treatments when quantified at a single timepoint in the summer (June, Bialic-Murphy et al., 2021; Burke et al., 2019) (Table 1).

Gas exchange measurements and calculations

Gas exchange measurements were collected from fully expanded leaves of two perennial understory native species: *Trillium* spp. (*Trillium grandiflorum* (Michx.) Salisb and *Trillium erectum* L.) and *Maianthemum racemosum* L. Link. We use *Trillium* spp. to refer to *T. grandiflorum* and *T. erectum*, as these species are difficult to distinguish if they are not reproductive. *Trillium* spp. and *M. racemosum* are understory perennial herbs that form rhizomes (i.e., geophytes), with widespread distributions in temperate forests of North America (USDA NRCS, 2022). Both species associate with AM fungi (Brundrett & Kendrick, 1987, 1990; Burke, 2008).

Gas exchange data were collected (n = 32 individuals for *Trillium* spp., n = 33 individuals for *M. racemosum*; Table 2) from three of the five experimental plots. Two plots were excluded due to an insufficient number of focal native species. Measurements were performed during two periods: once early in the growing season when the tree canopy was open and tree canopy leaf out was occurring (April 19 through April 21 for *Trillium* spp. and May 5 through May 6 for *M. racemosum*) and once later in the growth season when the tree canopy was fully closed (June 12 through June 15 for both species). The first measurement period was conducted at different time points for *Trillium* spp. and *M. racemosum* because of differences in the timing of full leaf expansion between the two species (Heberling et al., 2019).

Net photosynthesis (A_{net}; μmol m^{-2} s^{-1}), stomatal conductance (g_{sw}; mol m^{-2} s^{-1}), and intercellular CO_2 (C_i; μmol mol^{-1}) concentrations were measured across a range of atmospheric CO_2 concentrations (i.e., an A_{net}/C_i curve) using the Dynamic Assimilation™ Technique (Saathoff & Welles, 2021). This technique allows for high-throughput A_{net}/C_i curves that correspond well with steady-state methods in herbaceous species (Tejera-Nieves et al., 2024). We initiated each A_{net}/C_i curve after net photosynthesis and stomatal conductance reached stability in a LI-6800 cuvette where the flow rate was set to 500 mol s^{-1}, the mixing fan was set to 10000 rpm, vapor pressure deficit was set to 1.5 kPa, leaf temperature was set to 25°C, incoming light radiation was set to 2000 μmol m^{-2} s^{-1}, and the reference CO_2 concentration was set to 420 μmol mol^{-1} CO_2. After stability was achieved, we ramped the reference CO_2 down to 20 μmol mol^{-1} CO_2. The reference CO_2 then returned to 420 μmol mol^{-1} CO_2, where fluxes were allowed to stabilize for 90 seconds before beginning a ramp up to 1620 μmol mol^{-1} CO_2. Each reference CO_2 ramp was done at a rate of 200 μmol mol^{-1} min^{-1}, with logging intervals set to every five seconds. The initial measurement of each A_{net}/C_i curve was used to extract snapshot A_{net} and g_{sw} measurements.

A_{net}/Ci curve fitting and parameter estimation

We fit A_{net}/C_i curves using the 'fitaci' function in the 'plantecophys' R package (Duursma, 2015). This function estimates the maximum rate of Rubisco carboxylation (V_{cmax}; μmol m^{-2} s^{-1}) and maximum rate of electron transport for RuBP regeneration (J_{max}; μmol m^{-2} s^{-1}) using the Farquhar et al. (1980) model for C_3 photosynthesis. Restrictions on triose phosphate utilization (TPU) were included as an additional rate-limiting step in all curve fits and the temperature

standardization default in the function was turned off. Dark respiration was estimated in each curve fit as a fixed proportion of V_{cmax}. We used leaf temperature (T_{leaf}; in K) of each response curve to calculate Michaelis-Menten coefficients for Rubisco affinity to CO_2 (K_c; μmol mol^{-1}) and O_2 (K_o; mmol mol^{-1}), and the CO_2 compensation point (Γ^*; μmol mol^{-1}), following Bernacchi et al. (2001):

$$K_c = 404.9 * exp^{\left(\frac{79430(T_{leaf}-298)}{298RT_{leaf}}\right)} \quad (1)$$

$$K_o = 278.4 * exp^{\left(\frac{36380(T_k-298)}{298RT_{leaf}}\right)} \quad (2)$$

$$\Gamma^* = 42.75 * exp^{\left(\frac{37830(T_k-298)}{298RT_{leaf}}\right)} \quad (3)$$

T_{leaf}

where R is the universal gas constant (8.314 J mol^{-1} K^{-1}). All curves were visually inspected for goodness-of-fit before extracting V_{cmax} and J_{max} estimates for hypothesis testing.

For all A_{net}/C_i curve fits, we standardized V_{cmax} and J_{max} to 25°C (referenced as V_{cmax25} and J_{max25}) using a modified Arrhenius equation. Temperature-standardized V_{cmax} and J_{max} are referenced as V_{cmax25} and J_{max25} from this point forward. This temperature standardization removed the influence of enzyme kinetics on V_{cmax} and J_{max}, and, thus, reflected biochemical investment in the different underlying processes (Way & Yamori, 2014). Rate estimates were standardized to 25°C using the formulation presented in Kattge and Knorr (2007):

$$k_{standardized} = \frac{k_{observed}}{e^{\left[\frac{H_a\left(T_{leaf}-T_{standardized}\right)}{T_{standardized}RT_{leaf}}\right]} \times \frac{1+e^{\left(\frac{T_{standardized}\Delta S-H_d}{RT_{standardized}}\right)}}{1+e^{\left(\frac{T_{leaf}\Delta S-H_d}{RT_{leaf}}\right)}}} \quad (4)$$

$k_{standardized}$ is the temperature-standardized estimate of V_{cmax25} or J_{max25}, $k_{observed}$ is the temperature-unstandardized V_{cmax} or J_{max} estimate. H_a is the activation energy of V_{cmax} or J_{max} set to 71,513 J mol^{-1} for V_{cmax} or 49,884 J mol^{-1} or J_{max} (Kattge & Knorr, 2007). H_d is set to 200,000 J mol^{-1} and is the deactivation energy of both V_{cmax} and J_{max} (Medlyn et al., 2002). $T_{standardized}$ is the standardized leaf temperature of 25°C converted to 298.15 K. ΔS is an entropy term (J mol^{-1} $°C^{-1}$) that Kattge and Knorr (2007) calculated using a linear relationship with acclimated growth temperature (T_g, °C), where:

$$\Delta S_{vcmax} = -1.07T_g + 668.39 \quad (5)$$

and:

$$\Delta S_{jmax} = -0.75T_g + 659.70 \quad (6)$$

We estimated T_g as the mean temperature of the seven days leading up to each A_{net}/C_i curve, following that photosynthetic acclimation typically occurs along this timescale (as found in Smith and Dukes, 2018). Mean daily air temperature was estimated using data collected at a nearby weather station (station ID: USW000114762; coordinates: 40.355° N, 79.921° W) included in the Global Historical Climatology Network - Daily data product (Menne et al., 2012). V_{cmax25} and J_{max25} estimates were used to calculate the ratio of J_{max25} to V_{cmax25} (J_{max25}:V_{cmax25}; unitless) as an index of relative investment in electron transport for RuBP regeneration versus Rubisco carboxylation.

Stomatal limitation

The extent by which stomatal conductance limited net photosynthesis (unitless) was calculated following the approach described in Farquhar and Sharkey (1982), where:

$$Stomatal\ limitation = 1 - \frac{A_{net}}{A_{mod}} \quad (7)$$

A_{net} represents the measured net photosynthesis rate where atmospheric CO_2 is 420 μmol mol^{-1}. A_{mod} represents a theoretical photosynthetic rate where $C_i = C_a = 420$ μmol mol^{-1} (that is, no stomatal resistance to gas exchange), calculated as:

$$A_{mod} = V_{cmax}\frac{C_{i,mod} - \Gamma^*}{C_{i,mod} + K_m} - R_d \quad (8)$$

where V_{cmax} is the measured maximum rate of Rubisco carboxylation (i.e., not temperature-standardized to 25°C), $C_{i,mod}$ is the intercellular CO_2 concentration where $C_i = C_a$, set to 420 μmol mol^{-1}, Γ^* (μmol mol^{-1}) is the CO_2 compensation point in the absence of dark respiration, K_m is the Michaelis-Menten coefficient for Rubisco-limited photosynthesis (μmol mol^{-1}), and R_d is the dark respiration rate, estimated as a fixed proportion of V_{cmax}. K_m was calculated as:

$$K_m = K_c * \left(1 + \frac{O_i}{K_o}\right) \quad (9)$$

where K_c and K_o were calculated following Eqns. 1 and 2, respectively, while O_i is the leaf intercellular O_2 concentration, set to 210 μmol mol^{-1}.

Chlorophyll fluorescence measurements

Relative chlorophyll content (unitless, not calibrated to actual chlorophyll content), was measured after each A_{net}/C_i curve on the same leaf using a SPAD-meter built into a MultispeQ V2.0 handheld device (PhotosynQ Inc., East Lansing, MI, USA).

Soil characteristics

To characterize plant-available nitrogen and phosphorus at the time of leaf gas exchange measurements, resin strips (Membranes International Inc., Ringwood, NJ, USA) were placed approximately 10 cm below the soil surface to quantify mobile ammonium (ppm), nitrate (ppm), and phosphate (ppm) concentrations in each plot. An initial batch of resin strips was incubated in the field between April 19 and June 1, 2023, followed by a second batch inserted in the same plot location between May 30 and June 29, 2023. A total of 36 strips, 12 for each nutrient, were placed in each plot to account for the high degree of spatial heterogeneity of soil nutrient availability in temperate forests (Akana et al., 2023). Cation and anion concentrations were extracted from resin strips in 0.5 M potassium sulfate at a 1:5 dilution factor for ammonium, and nitrate, and 1 M HCl for phosphate. Concentrations of each nutrient were determined through end products of standard colorimetric reactions (D'Angelo et al., 2001; Doane & Horwáth, 2003; Lajtha et al., 1999; Weatherburn, 1967). Soil inorganic nitrogen availability was estimated as the sum of the ammonium and nitrate concentrations. The soil inorganic nitrogen-to-phosphorus ratio was estimated as the ratio of soil inorganic nitrogen availability to soil phosphate availability.

Soil moisture data were collected using TOMST® TMS-4 data loggers (TOMST® s.r.o., Prague, Czech Republic). One data logger was placed in each *A. petiolata* treatment of each plot (i.e., 2 data loggers per plot) on April 26, 2023 and recorded soil moisture pulses every 15 minutes. Volumetric soil moisture content (%) was calculated using the calibration curves for a silt loam soil reported in Wild et al. (2019). We calculated the mean daily volumetric soil moisture content and used these values as the primary indicator of soil moisture throughout the measurement period.

Data analysis

We built a series of linear mixed-effects models to explore the effects of *A. petiolata* treatment and measurement period on soil nutrient availability. Each model included *A. petiolata* treatment

(ambient, weeded) and measurement period (open, closed tree canopy) as fixed effects, with an additional interaction term between *A. petiolata* treatment and measurement period. Plot was included as a random intercept term. We constructed separate models with this independent variable structure for soil nitrate availability, soil ammonium availability, soil inorganic nitrogen (nitrate + ammonium) availability, soil phosphate availability, and the soil nitrogen-to-phosphorus ratio. The models for soil inorganic nitrogen availability and the soil nitrogen-to-phosphorus ratio were fitted using dependent variables that were natural-log transformed, while the model for soil ammonium availability was fitted after soil ammonium availability was square root-transformed to normalize model residuals (Shapiro-Wilk: $p>0.05$ in all cases).

Next, we built a linear mixed-effects model to explore the effect of *A. petiolata* treatment on volumetric soil moisture content across the measurement period. This model included *A. petiolata* treatment (ambient levels, weeded) and day of year (continuous) as fixed effects, with an added interaction term between *A. petiolata* treatment and day of year. Plot was included as a random intercept term.

Finally, we built a series of species-specific linear mixed-effects models to explore the effect of *A. petiolata* treatment and measurement period on leaf physiological traits of *Trillium* spp. and *M. racemosum*. Species were not concatenated into a single linear mixed-effect model for each trait because we did not seek to understand interspecies variability in measured traits. All models included *A. petiolata* treatment (ambient, weeded) and measurement period (open, closed tree canopy) as fixed effects, as well as an interaction term between *A. petiolata* treatment and measurement period. Plot was included as a random intercept term. Plant individual was also included as a random intercept term to account for repeated measures. Individuals were only included in analyses if gas exchange measurements were collected during both measurement periods. We constructed separate models with this independent variable structure for each species for the following dependent variables: A_{net}, g_{sw}, stomatal limitation, V_{cmax25}, J_{max25}, J_{max25}:V_{cmax25}, and SPAD. Models for A_{net}, g_{sw}, V_{cmax25}, and J_{max25} in *Trillium* spp. were fitted using dependent variables that were natural-log transformed to normalize model residuals, while models for stomatal limitation, *SPAD*, and J_{max25} in *M. racemosum* were fitted using dependent variables that were natural-log transformed to normalize model residuals (Shapiro-Wilk: $p>0.05$ in all cases).

Each model was fitted using the 'lmer' function in the 'lme4' R package (Bates *et al.*, 2015). Type II Wald's χ^2 and the significance (α=0.05) of each fixed effect coefficient was calculated using the 'Anova' function in the 'car' R package (Fox & Weisberg, 2019). We used the 'emmeans' R package (Lenth, 2019) to conduct post hoc comparisons using Tukey's tests, where degrees of freedom were approximated using the Kenward-Roger approach (Kenward & Roger, 1997). All analyses and plots were conducted in R version 4.1.0 (R Core Team, 2021). Data, analysis scripts, and plot scripts are available on Zenodo (DOI: 10.5281/13862911).

Results

Soil characteristics

Resin strips collected after tree canopy closure had significantly lower soil inorganic nitrogen availability (p<0.001, Table 3; Fig. 1a) and soil phosphate availability (p=0.001, Table 3; Fig. 1b) compared to those collected before tree canopy closure, decreasing the soil nitrogen-to-phosphorus ratio (p<0.001, Table 3; Fig. 1c). Soil nitrate availability was lower after tree canopy closure (p<0.001, Table 3; Fig. S1), while soil ammonium availability was unaffected by canopy status (p=0.770, Table 3; Fig. S1).

Alliaria petiolata treatment had no effect on soil inorganic nitrogen availability (p=0.104, Table 3; Fig. 1a), soil phosphate availability (p=0.108, Table 3; Fig. 1b), soil ammonium availability (p=0.845, Table 3; Fig. S1), or soil nitrate availability (p=0.106, Table 3; Fig. S1). However, the soil nitrogen-to-phosphorus ratio was marginally greater in the *A. petiolata*-ambient treatment compared to the *A. petiolata*-weeded treatment (p=0.078, Table 3; Fig. 1c) due to an insignificant increase in soil inorganic nitrogen availability (p=0.104, Table 3) and insignificant decrease in soil phosphate availability (p=0.106, Table 3; Fig. 1b).

Soil moisture decreased as the growth season progressed (p<0.001; Table 3; Fig. 1d) and was lower in the *A. petiolata*-ambient than the *A. petiolata*-weeded treatment (p<0.001; Table 3; Fig. 1d). There was no interaction between *A. petiolata* treatment and day of year (p=0.602; Table 3; Fig. 1d).

Gas exchange

For *Trillium* spp., measurements collected after tree canopy closure demonstrated significantly reduced net photosynthesis and stomatal conductance rates and significantly greater stomatal

limitation compared to measurements collected before tree canopy closure (p<0.001 in all cases, Table 4; Fig. 2a, 2c, 2e). Net photosynthesis was marginally reduced in the *A. petiolata*-ambient treatment compared to the *A. petiolata*-weeded treatment (p=0.064, Table 4; Fig. 2a), with amplified responses observed after canopy closure (*A. petiolata* treatment-by-canopy status interaction: p=0.032, Table 4; Fig. 2a). *Alliaria petiolata* treatment had no effect on stomatal conductance (p=0.726, Table 4; Fig. 2c) or stomatal limitation (p=0.751, Table 4; Fig. 2e), regardless of canopy status (*A. petiolata* treatment-by-canopy status interaction: p>0.05 in both cases, Table 4).

For *M. racemosum*, measurements collected after canopy closure exhibited significantly reduced net photosynthesis and stomatal conductance rates and significantly greater stomatal limitation compared to measurements collected before canopy closure (p<0.001 in all cases, Table 4; Fig. 2b, 2d, 2f). In the *A. petiolata*-ambient treatment, net photosynthesis and stomatal conductance rates each significantly decreased (p=0.016 for net photosynthesis, p=0.002 for stomatal conductance, Table 4) while stomatal limitation significantly increased (p=0.007, Table 4) compared to the *A. petiolata*-weeded treatment. For net photosynthesis and stomatal conductance, these responses were independent of *A. petiolata* treatment (*A. petiolata*-by-canopy interaction: p>0.05 in both cases; Table 4; Fig. 2b, 2d). Stomatal limitation responses to *A. petiolata* were amplified after canopy closure (*A. petiolata*-by-canopy interaction: p=0.023; Table 4; Fig. 2f).

Relative chlorophyll content

SPAD values were greater in *Trillium* spp. and *M. racemosum* for measurements collected after canopy closure (p<0.001 in both cases, Table 4; Fig. S2). *Alliaria petiolata* treatment had no effect on SPAD in either species (p>0.05 in both cases, Table 4) regardless of canopy status (*A. petiolata*-by-canopy interaction: p>0.05 in both cases; Table 4).

Photosynthetic capacity

In *Trillium* spp., measurements collected after canopy closure exhibited significantly decreased V_{cmax25} and J_{max25} compared measurements collected before canopy closure (p<0.001 in both cases, Table 5; Fig. 3a, 3c), resulting in a significant increase in J_{max25}:V_{cmax25} following canopy closure (p=0.007; Table 5; Fig. 3e). In the *A. petiolata*-ambient treatment, V_{cmax25} was unaffected

(p=0.139; Table 5) while J_{max25} was significantly reduced (p=0.021; Table 5) compared to the *A. petiolata*-weeded treatment, leading to a marginal decline in J_{max25}:V_{cmax25} (p=0.052; Table 5; Fig. 3e). A significant interaction between *A. petiolata* treatment and canopy status for V_{cmax25} (p=0.032; Table 5; Fig. 3a) and J_{max25} (p=0.014; Table 5; Fig. 3c) indicated amplified *A. petiolata* effects after tree canopy closure.

For *M. racemosum*, measurements collected after canopy closure demonstrated significantly decreased V_{cmax25} and J_{max25} compared to measurements collected before canopy closure (p<0.001 in both cases, Table 5; Fig. 3b, 3d). J_{max25}:V_{cmax25} was not altered by canopy status (p=0.335, Table 5; Fig. 3f). *Alliaria petiolata* treatment had no effect on V_{cmax25} (p=0.992, Table 5), J_{max25} (p=0.948, Table 5), or J_{max25}:V_{cmax25} (p=0.671, Table 5) regardless of canopy status (*A. petiolata* treatment-by-canopy status interaction: p>0.05 all cases; Table 5).

Discussion

Alliaria petiolata presence decreased net photosynthesis rates in both native understory species tested. This response was strongest in *Trillium* spp. after tree canopy closure and was consistently observed across the growing season in *M. racemosum*. Reduced net photosynthesis rates in both species were affected by contrasting mechanisms: decreased apparent temperature-standardized photosynthetic capacity in *Trillium* spp. and reduced stomatal conductance in *M. racemosum*. Together, these findings highlight the need to understand species-specific responses to allelopathic invaders and other anthropogenic stressors to natural ecosystems, and to consider the temporal changes in the expression of native plant physiologies. In this system, these findings also provide a physiological mechanism that may help to understand how the effects of *A. petiolata* on AM fungal mutualism disruption could scale to native plant population and community dynamics (Table 1).

Photosynthetic responses to A. petiolata presence are linked to altered nutrient and water economics

Both native species growing under ambient levels of *A. petiolata* exhibited significantly reduced net photosynthesis rates compared to those growing in the *A. petiolata*-weeded treatment, supporting our first hypothesis. In *Trillium* spp., this response was associated with a reduction in J_{max25}, but no change in V_{cmax25}, stomatal conductance, or stomatal limitation. These patterns are

indicative of increased photosynthetic nutrient stress and no apparent sign of water stress. The J_{max25} response, coupled with marginally greater soil N:P in *A. petiolata*-ambient plots, indicates that *A. petiolata* may have induced phosphorus stress (Domingues et al., 2010). In contrast, reduced net photosynthesis in *M. racemosum* was associated with a reduction in stomatal conductance, an increase in stomatal limitation, and no change in V_{cmax25} or J_{max25}. These patterns indicate that *A. petiolata* presence induced water stress without signs of nutrient stress. Increased water stress in *M. racemosum* could reflect greater plot-level water demand in the *A. petiolata*-ambient treatment, where presence of *A. petiolata* may have increased plant density and thus community-level water uptake compared to weeded plots. However, *Trillium* spp. did not exhibit these water stress signatures, and similar net photosynthesis and stomatal conductance patterns were observed in a controlled greenhouse experiment under well-watered conditions (Hale et al., 2016). These patterns corresponded with null effects of *A. petiolata* treatment on apparent photosynthetic capacity, consistent with previous work showing that *M. racemosum* responses to *A. petiolata* invasion are associated with changes in water, not nutrient, economics (Hale et al., 2011, 2016).

Contrasting mechanisms that defined the physiological responses of *Trillium* spp. and *M. racemosum* to *A. petiolata* may be explained through the lens of the leaf economics spectrum (Reich, 2014; Wright et al., 2004). While *Trillium* spp. and *M. racemosum* share many functional and ecological traits, such as rhizome formation, clonal reproduction, nutrient and water acquisition through direct uptake pathways or symbioses with AM fungi, and similar spring emergence times (Brundrett & Kendrick, 1987, 1990; Heberling et al., 2019), these two species differ in leaf lifespan (Heberling et al., 2019), placing them at different positions along the leaf economics spectrum (Onoda et al., 2017; Reich, 2014; Wright et al., 2004). Relatively short-lived *Trillium* spp. leaves require rapid nutrient uptake to support faster growth and reproduction, whereas longer-lived *M. racemosum* leaves may adopt resource-conservative strategies that depend on sustained water use. Consistent with this hypothesis, *M. racemosum* exhibited lower V_{cmax25} on average than *Trillium* (V_{cmax25} mean±SD: 44.4±19.1 μmol m^{-2} s^{-1} in *M. racemosum*, 65.3±41.8 μmol m^{-2} s^{-1} in *Trillium* spp.), reflecting its more conservative strategy. Tracer studies that quantify nutrient and water usage may be needed to verify whether this is the case.

Photosynthetic responses to A. petiolata presence are strongest after tree canopy closure

Contrary to our second hypothesis, *A. petiolata* treatment effects on leaf-level photosynthetic traits were largely absent early in the season when understory demand for soil resources was presumed to be the greatest. This null response may be attributed to resource optimization that caused individuals in both treatments to favor investment toward direct uptake. Resource optimization theory predicts that, given multiple potential acquisition strategies (e.g., direct uptake, mycorrhizal symbioses, etc.), plants should prioritize investment toward the resource uptake strategy that minimizes the cost and maximizes the uptake efficiency of acquiring soil resources (Bloom et al., 1985; Kummel & Salant, 2006; Rastetter et al., 2001). Thus, plants should invest in direct uptake pathways early in the growing season when soil resources are more abundant, as costs to acquire soil resources through direct uptake pathways are often reduced under high resource availability (Lu et al., 2022; Perkowski et al., 2021, 2024). Null photosynthetic responses early in the growing season may have been due to investment toward direct uptake that allowed individuals to satisfy photosynthetic demand to build enzymes and maintain transpiration while minimizing any negative consequence of relying on disrupted AM fungal partners for resources.

Supporting our second hypothesis, the effects of *A. petiolata* treatment on leaf-level photosynthetic traits were often stronger after tree canopy closure. For *Trillium* spp., interactions between *A. petiolata* and canopy closure for net photosynthesis, V_{cmax25}, and J_{max25} indicated that *A. petiolata* had stronger negative effects on these traits after canopy closure. For *M. racemosum*, temporal effects of *A. petiolata* on photosynthetic traits were less clear. Positive effects of *A. petiolata* on stomatal limitation were indeed stronger after tree canopy closure; however, canopy status did not modify net photosynthesis and stomatal conductance responses to *A. petiolata*. Regardless, canopy closure strongly covaried with a reduction in soil nitrogen availability, soil phosphorus availability, and soil moisture. Given this, stronger late-season photosynthetic responses to *A. petiolata* treatment may have been due to increased reliance on disrupted AM fungal partners as the cost to acquire resources through direct uptake increased (Perkowski et al., 2021, 2024). This may have been further exacerbated by a reduction in soil moisture in the *A. petiolata*-ambient treatment and may have also been indicative of increased phosphorus limitation. Strong covariance between canopy closure and soil resource availability limits our ability to ascertain whether plant responses to *A. petiolata* were driven by the reduction in light availability or soil resource availability. Additionally, we did not explicitly assess the link

between AM fungal mutualism disruption and native plant physiology responses to *A. petiolata*, which is an important next step toward understanding how soil microbial community disruption due to allelopathic invaders scale to impact native plant physiology and community composition. Specifically, isotopic tracers (e.g., Hodge & Fitter, 2010) or soil resource manipulation experiments across different AM fungal communities (e.g., Gustafson & Casper, 2004) would be a useful next step for linking soil microbial community, soil resource availability, and photosynthetic responses of native species to allelopathic invaders.

Overall, these findings highlight the necessity of quantifying the temporal effects of plant invasion on coexisting native plant populations. Ecophysiological studies have traditionally focused on the impacts of allelopathic invaders on the physiological processes of native species at single timepoints. While results from that approach provide a snapshot of plant invader effects on native populations' physiology, assuming that they represent native physiology across the growing season can be misleading. This risk may be especially important in systems where light availability is a function of tree canopy closure and soil resource availability declines across the growing season. Experiments that assess the impacts of plant invasion across more than one timepoint, as reported here, can provide important insight into physiological mechanisms that underpin the effects of plant invasion on native populations. Further, they provide important empirical data that improves our ability to reliably predict how plant invasion scales up to plant population and community dynamics. Finally, soil microbial and plant communities operate on largely different spatiotemporal scales, which poses a challenge when scaling soil microbial community changes up to plant community dynamics. Quantifying differential physiological responses across the growing season by coexisting native plant species in the context of community invasion may allow us to integrate and scale the effects of plant invasions on belowground soil microbial and plant community dynamics. Indeed, our results indicate that photosynthetic responses to *A. petiolata* are directionally similar to its impacts on AM fungal community and plant community dynamics (Table 1), suggesting that the effects of *A. petiolata* invasion may be inherently scalable through its impacts on native plant physiology.

References

Akana, P. R., Mifsud, I. E. J., & Menge, D. N. L. (2023). Soil nitrogen availability in a temperate forest exhibits large variability at sub-tree spatial scales. *Biogeochemistry*, *164*(3), 537–553. https://doi.org/10.1007/s10533-023-01056-5

Ali, A. A., Xu, C., Rogers, A., McDowell, N. G., Medlyn, B. E., Fisher, R. A., Wullschleger, S. D., Reich, P. B., Vrugt, J. A., Bauerle, W. L., Santiago, L. S., & Wilson, C. J. (2015). Global-scale environmental control of plant photosynthetic capacity. *Ecological Applications*, *25*(8), 2349–2365. https://doi.org/10.1890/14-2111.1

Anthony, M. A., Stinson, K. A., Trautwig, A. N., Coates-Connor, E., & Frey, S. D. (2019). Fungal communities do not recover after removing invasive *Alliaria petiolata* (garlic mustard). *Biological Invasions*, *21*(10), 3085–3099. https://doi.org/10.1007/s10530-019-02031-8

Bernacchi, C. J., Singsaas, E. L., Pimentel, C., Portis, A. R., & Long, S. P. (2001). Improved temperature response functions for models of Rubisco-limited photosynthesis. *Plant, Cell and Environment*, *24*(2), 253–259. https://doi.org/10.1046/j.1365-3040.2001.00668.x

Bialic-Murphy, L., Brouwer, N. L., & Kalisz, S. (2020). Direct effects of a non-native invader erode native plant fitness in the forest understory. *Journal of Ecology*, *108*(1), 189–198. https://doi.org/10.1111/1365-2745.13233

Bialic-Murphy, L., Smith, N. G., Voothuluru, P., McElderry, R. M., Roche, M. D., Cassidy, S. T., Kivlin, S. N., & Kalisz, S. (2021). Invasion-induced root–fungal disruptions alter plant water and nitrogen economies. *Ecology Letters*, *24*(6), 1145–1156. https://doi.org/10.1111/ele.13724

Bloom, A. J., Chapin, F. S., & Mooney, H. A. (1985). Resource limitation in plants-an economic analogy. *Annual Review of Ecology and Systematics*, *16*(1), 363–392. https://doi.org/10.1146/annurev.es.16.110185.002051

Brouwer, N. L., Hale, A. N., & Kalisz, S. (2015). Mutualism-disrupting allelopathic invader drives carbon stress and vital rate decline in a forest perennial herb. *AoB PLANTS*, *7*(1), 1–14. https://doi.org/10.1093/aobpla/plv014

Brundrett, M. C., & Kendrick, B. (1987). The mycorrhizal status, root anatomy, and phenology of plants in a sugar maple forest. *Canadian Journal of Botany*, *66*, 1153–1173.

Brundrett, M. C., & Kendrick, B. (1990). The roots and mycorrhizas of herbaceous woodland plants: I. Quantitative aspects of morphology. *New Phytologist*, *114*(3), 457–468. https://doi.org/10.1111/j.1469-8137.1990.tb00415.x

Burke, D. J. (2008). Effects of *Alliaria petiolata* (garlic mustard; Brassicaceae) on mycorrhizal colonization and community structure in three herbaceous plants in a mixed deciduous forest. *American Journal of Botany*, *95*(11), 1416–1425. https://doi.org/10.3732/ajb.0800184

Burke, D. J., Carrino-Kyker, S. R., Hoke, A., Cassidy, S., Bialic-Murphy, L., & Kalisz, S. (2019). Deer and invasive plant removal alters mycorrhizal fungal communities and soil chemistry: Evidence from a long-term field experiment. *Soil Biology and Biochemistry*, *128*(September 2018), 13–21. https://doi.org/10.1016/j.soilbio.2018.09.031

Burke, D. J., Weintraub, M. N., Hewins, C. R., & Kalisz, S. (2011). Relationship between soil enzyme activities, nutrient cycling and soil fungal communities in a northern hardwood forest. *Soil Biology and Biochemistry*, *43*(4), 795–803. https://doi.org/10.1016/j.soilbio.2010.12.014

Callaway, R. M., Cipollini, D., Barto, K., Thelen, G. C., Hallett, S. G., Prati, D., Stinson, K., & Klironomos, J. (2008). Novel weapons: Invasive plant suppresses fungal mutualists in America but not in its native Europe. *Ecology*, *89*(4), 1043–1055. https://doi.org/10.1890/07-0370.1

565 Callaway, R. M., & Ridenour, W. M. (2004). Novel weapons: Invasive success and the evolution
566 of increased competitive ability. *Frontiers in Ecology and the Environment*, *2*(8), 436–443.
567 https://doi.org/10.1890/1540-9295(2004)002[0436:NWISAT]2.0.CO;2
568 Cantor, A., Hale, A., Aaron, J., Traw, M. B., & Kalisz, S. (2011). Low allelochemical
569 concentrations detected in garlic mustard-invaded forest soils inhibit fungal growth and
570 AMF spore germination. *Biological Invasions*, *13*(12), 3015–3025.
571 https://doi.org/10.1007/s10530-011-9986-x
572 D'Angelo, E., Crutchfield, J., & Vandiviere, M. (2001). Rapid, sensitive, microscale
573 determination of phosphate in water and soil. *Journal of Environmental Quality*, *30*(6),
574 2206–2209. https://doi.org/10.2134/jeq2001.2206
575 Doane, T. A., & Horwáth, W. R. (2003). Spectrophotometric determination of nitrate with a
576 single reagent. *Analytical Letters*, *36*(12), 2713–2722. https://doi.org/10.1081/AL-
577 120024647
578 Domingues, T. F., Meir, P., Feldpausch, T. R., Saiz, G., Veenendaal, E. M., Schrodt, F., Bird,
579 M., Djagbletey, G., Hien, F., Compaore, H., Diallo, A., Grace, J., & Lloyd, J. (2010). Co-
580 limitation of photosynthetic capacity by nitrogen and phosphorus in West Africa
581 woodlands. *Plant, Cell and Environment*, *33*(6), 959–980. https://doi.org/10.1111/j.1365-
582 3040.2010.02119.x
583 Duursma, R. A. (2015). Plantecophys - an R package for analysing and modelling leaf gas
584 exchange data. *PLOS ONE*, *10*(11), e0143346.
585 https://doi.org/10.1371/journal.pone.0143346
586 Ellsworth, D. S., Crous, K. Y., De Kauwe, M. G., Verryckt, L. T., Goll, D., Zaehle, S.,
587 Bloomfield, K. J., Ciais, P., Cernusak, L. A., Domingues, T. F., Dusenge, M. E., Garcia, S.,
588 Guerrieri, R., Ishida, F. Y., Janssens, I. A., Kenzo, T., Ichie, T., Medlyn, B. E., Meir, P., …
589 Wright, I. J. (2022). Convergence in phosphorus constraints to photosynthesis in forests
590 around the world. *Nature Communications*, *13*(1), 5005. https://doi.org/10.1038/s41467-
591 022-32545-0
592 Evans, J. R. (1989). Photosynthesis and nitrogen relationships in leaves of C_3 plants. *Oecologia*,
593 *78*(1), 9–19. https://doi.org/10.1007/BF00377192
594 Evans, J. R., & Clarke, V. C. (2019). The nitrogen cost of photosynthesis. *Journal of*
595 *Experimental Botany*, *70*(1), 7–15. https://doi.org/10.1093/jxb/ery366
596 Evans, J. R., & Seemann, J. R. (1989). The allocation of protein nitrogen in the photosynthetic
597 apparatus: costs, consequences, and control. *Photosynthesis*, *8*, 183–205.
598 Farquhar, G. D., & Sharkey, T. D. (1982). Stomatal conductance and photosynthesis. *Annual*
599 *Review of Plant Physiology*, *33*(1), 317–345.
600 https://doi.org/10.1146/annurev.pp.33.060182.001533
601 Farquhar, G. D., von Caemmerer, S., & Berry, J. A. (1980). A biochemical model of
602 photosynthetic CO_2 assimilation in leaves of C_3 species. *Planta*, *149*(1), 78–90.
603 https://doi.org/10.1007/BF00386231
604 Fox, J., & Weisberg, S. (2019). *An R companion to applied regression* (Third edit). Sage.
605 https://socialsciences.mcmaster.ca/jfox/Books/Companion/
606 Gustafson, D. J., & Casper, B. B. (2004). Nutrient addition affects AM fungal performance and
607 expression of plant/fungal feedback in three serpentine grasses. *Plant and Soil*, *259*(1–2), 9–
608 17. https://doi.org/10.1023/B:PLSO.0000020936.56786.a4

609 Hale, A. N., & Kalisz, S. (2012). Perspectives on allelopathic disruption of plant mutualisms: A
610 framework for individual- and population-level fitness consequences. *Plant Ecology*,
611 *213*(12), 1991–2006. https://doi.org/10.1007/s11258-012-0128-z
612 Hale, A. N., Lapointe, L., & Kalisz, S. (2016). Invader disruption of belowground plant
613 mutualisms reduces carbon acquisition and alters allocation patterns in a native forest herb.
614 *New Phytologist*, *209*(2), 542–549. https://doi.org/10.1111/nph.13709
615 Hale, A. N., Tonsor, S. J., & Kalisz, S. (2011). Testing the mutualism disruption hypothesis:
616 physiological mechanisms for invasion of intact perennial plant communities. *Ecosphere*,
617 *2*(10), art110. https://doi.org/10.1890/es11-00136.1
618 Heberling, J. M., Cassidy, S. T., Fridley, J. D., & Kalisz, S. (2019). Carbon gain phenologies of
619 spring-flowering perennials in a deciduous forest indicate a novel niche for a widespread
620 invader. *New Phytologist*, *221*(2), 778–788. https://doi.org/10.1111/nph.15404
621 Hodge, A., & Fitter, A. H. (2010). Substantial nitrogen acquisition by arbuscular mycorrhizal
622 fungi from organic material has implications for N cycling. *Proceedings of the National*
623 *Academy of Sciences*, *107*(31), 13754–13759.
624 Hungate, B. A., Dukes, J. S., Shaw, M. R., Luo, Y., & Field, C. B. (2003). Nitrogen and climate
625 change. *Science*, *302*(5650), 1512–1513. https://doi.org/10.1126/science.1091390
626 Inderjit, Wardle, D. A., Karban, R., & Callaway, R. M. (2011). The ecosystem and evolutionary
627 contexts of allelopathy. *Trends in Ecology and Evolution*, *26*(12), 655–662.
628 https://doi.org/10.1016/j.tree.2011.08.003
629 Kalisz, S., Kivlin, S. N., & Bialic-Murphy, L. (2021). Allelopathy is pervasive in invasive plants.
630 *Biological Invasions*, *23*(2), 367–371. https://doi.org/10.1007/s10530-020-02383-6
631 Kattge, J., & Knorr, W. (2007). Temperature acclimation in a biochemical model of
632 photosynthesis: a reanalysis of data from 36 species. *Plant, Cell & Environment*, *30*(9),
633 1176–1190. https://doi.org/10.1111/j.1365-3040.2007.01690.x
634 Kenward, M. G., & Roger, J. H. (1997). Small sample inference for fixed effects from restricted
635 maximum likelihood. *Biometrics*, *53*(3), 983. https://doi.org/10.2307/2533558
636 Kummel, M., & Salant, S. W. (2006). The economics of mutualisms: Optimal utilization of
637 mycorrhizal mutualistic partners by plants. *Ecology*, *87*(4), 892–902.
638 https://doi.org/10.1890/0012-9658(2006)87[892:TEOMOU]2.0.CO;2
639 Lajtha, K., Driscoll, C. T., Jarrell, W. M., & Elliott, E. T. (1999). Soil phosphorus. In *Standard*
640 *Soil Methods for Long-Term Ecological Research* (p. 115).
641 Lenth, R. (2019). *emmeans: estimated marginal means, aka least-squares means*. https://cran.r-
642 project.org/package=emmeans
643 Lu, J., Yang, J., Keitel, C., Yin, L., Wang, P., Cheng, W., & Dijkstra, F. A. (2022). Belowground
644 carbon efficiency for nitrogen and phosphorus acquisition varies between *Lolium perenne*
645 and *Trifolium repens* and depends on phosphorus fertilization. *Frontiers in Plant Science*,
646 *13*, 1–9. https://doi.org/10.3389/fpls.2022.927435
647 Medlyn, B. E., Dreyer, E., Ellsworth, D. S., Forstreuter, M., Harley, P. C., Kirschbaum, M. U. F.,
648 Le Roux, X., Montpied, P., Strassemeyer, J., Walcroft, A., Wang, K., & Loustau, D. (2002).
649 Temperature response of parameters of a biochemically based model of photosynthesis. II.
650 A review of experimental data. *Plant, Cell & Environment*, *25*(9), 1167–1179.
651 https://doi.org/10.1046/j.1365-3040.2002.00891.x
652 Medrano, H., Escalona, J. M., Bota, J., Gulías, J., & Flexas, J. (2002). Regulation of
653 Photosynthesis of C3 Plants in Response to Progressive Drought: Stomatal Conductance as

a Reference Parameter. *Annals of Botany*, *89*(7), 895–905. https://doi.org/10.1093/aob/mcf079

Menne, M. J., Durre, I., Vose, R. S., Gleason, B. E., & Houston, T. G. (2012). An overview of the global historical climatology network-daily database. *Journal of Atmospheric and Oceanic Technology*, *29*(7), 897–910. https://doi.org/10.1175/JTECH-D-11-00103.1

Onoda, Y., Wright, I. J., Evans, J. R., Hikosaka, K., Kitajima, K., Niinemets, Ü., Poorter, H., Tosens, T., & Westoby, M. (2017). Physiological and structural tradeoffs underlying the leaf economics spectrum. *New Phytologist*, *214*(4), 1447–1463. https://doi.org/10.1111/nph.14496

Palecki, M., Durre, I., Applequist, S., Arguez, A., & Lawrimore, J. H. (2021). U.S. Climate Normals 2020: U.S. Hourly Climate Normals (1991-2020). *NOAA National Centers for Environmental Information*.

Perkowski, E. A., Ezekannagha, E., & Smith, N. G. (2025). Nitrogen demand, availability, and acquisition strategy control plant responses to elevated CO_2. *Journal of Experimental Botany*, *76*(10), 2908–2923. https://doi.org/10.1093/jxb/eraf118

Perkowski, E. A., Terrones, J., German, H. L., & Smith, N. G. (2024). Symbiotic nitrogen fixation reduces belowground biomass carbon costs of nitrogen acquisition under low, but not high, nitrogen availability. *AoB PLANTS*, *16*(5), 1–22. https://doi.org/10.1093/aobpla/plae051

Perkowski, E. A., Waring, E. F., & Smith, N. G. (2021). Root mass carbon costs to acquire nitrogen are determined by nitrogen and light availability in two species with different nitrogen acquisition strategies. *Journal of Experimental Botany*, *72*(15), 5766–5776. https://doi.org/10.1093/jxb/erab253

Qu, T., Du, X., Peng, Y., Guo, W., Zhao, C., & Losapio, G. (2021). Invasive species allelopathy decreases plant growth and soil microbial activity. *PLoS ONE*, *16*(2 February), 1–12. https://doi.org/10.1371/journal.pone.0246685

R Core Team. (2021). *R: A language and environment for statistical computing* (4.1.1). R Foundation for Statistical Computing. https://www.r-project.org/

Rastetter, E. B., Vitousek, P. M., Field, C. B., Shaver, G. R., Herbert, D., & Ågren, G. I. (2001). Resource optimization and symbiotic nitrogen fixation. *Ecosystems*, *4*(4), 369–388. https://doi.org/10.1007/s10021-001-0018-z

Reich, P. B. (2014). The world-wide 'fast-slow' plant economics spectrum: a traits manifesto. *Journal of Ecology*, *102*(2), 275–301. https://doi.org/10.1111/1365-2745.12211

Roche, M. D., Pearse, I. S., Bialic-Murphy, L., Kivlin, S. N., Sofaer, H. R., & Kalisz, S. (2021). Negative effects of an allelopathic invader on AM fungal plant species drive community-level responses. *Ecology*, *102*(1), 1–12. https://doi.org/10.1002/ecy.3201

Roche, M. D., Pearse, I. S., Sofaer, H. R., Kivlin, S. N., Spyreas, G., Zaya, D. N., & Kalisz, S. (2023). Invasion-mediated mutualism disruption is evident across heterogeneous environmental conditions and varying invasion intensities. *Ecography*, *2023*(7), 1–11. https://doi.org/10.1111/ecog.06434

Rodgers, V. L., Stinson, K. A., & Finzi, A. C. (2008). Ready or not, garlic mustard is moving in: *Alliaria petiolata* as a member of eastern north American forests. *BioScience*, *58*(5), 426–436. https://doi.org/10.1641/B580510

Saathoff, A. J., & Welles, J. (2021). Gas exchange measurements in the unsteady state. *Plant Cell and Environment*, *44*(11), 3509–3523. https://doi.org/10.1111/pce.14178

Smith, N. G., & Dukes, J. S. (2018). Drivers of leaf carbon exchange capacity across biomes at the continental scale. *Ecology*, *99*(7), 1610–1620. https://doi.org/10.1002/ecy.2370

Smith, S. E., & Read, D. J. (2008). *Mycorrhizal Symbiosis*.

Tejera-Nieves, M., Seong, D. Y., Reist, L., & Walker, B. J. (2024). The Dynamic Assimilation Technique measures photosynthetic CO_2 response curves with similar fidelity to steady-state approaches in half the time. *Journal of Experimental Botany*, *75*(10), 2819–2828. https://doi.org/10.1093/jxb/erae057

USDA NRCS. (2022). The PLANTS Database. *(Http://Plants.Usda.Gov, 18 November 2022). National Plant Data Team, Greensboro, NC 27401-4901 USA*.

Walker, A. P., Beckerman, A. P., Gu, L., Kattge, J., Cernusak, L. A., Domingues, T. F., Scales, J. C., Wohlfahrt, G., Wullschleger, S. D., & Woodward, F. I. (2014). The relationship of leaf photosynthetic traits - V_{cmax} and J_{max} - to leaf nitrogen, leaf phosphorus, and specific leaf area: a meta-analysis and modeling study. *Ecology and Evolution*, *4*(16), 3218–3235. https://doi.org/10.1002/ece3.1173

Waring, E. F., Perkowski, E. A., & Smith, N. G. (2023). Soil nitrogen fertilization reduces relative leaf nitrogen allocation to photosynthesis. *Journal of Experimental Botany*, *74*(17), 5166–5180. https://doi.org/10.1093/jxb/erad195

Way, D. A., & Yamori, W. (2014). Thermal acclimation of photosynthesis: on the importance of adjusting our definitions and accounting for thermal acclimation of respiration. *Photosynthesis Research*, *119*(1–2), 89–100. https://doi.org/10.1007/s11120-013-9873-7

Weatherburn, M. W. (1967). Phenol-hypochlorite reaction for determination of ammonia. *Analytical Chemistry*, *39*(8), 971–974. https://doi.org/10.1021/ac60252a045

Wild, J., Kopecký, M., Macek, M., Šanda, M., Jankovec, J., & Haase, T. (2019). Climate at ecologically relevant scales: A new temperature and soil moisture logger for long-term microclimate measurement. *Agricultural and Forest Meteorology*, *268*(July 2018), 40–47. https://doi.org/10.1016/j.agrformet.2018.12.018

Wright, I. J., Reich, P. B., Westoby, M., Ackerly, D. D., Baruch, Z., Bongers, F., Cavender-Bares, J., Chapin, T., Cornelissen, J. H. C., Diemer, M., Flexas, J., Garnier, E., Groom, P. K., Gulias, J., Hikosaka, K., Lamont, B. B., Lee, T. D., Lee, W., Lusk, C. H., … Villar, R. (2004). The worldwide leaf economics spectrum. *Nature*, *428*(6985), 821–827. https://doi.org/10.1038/nature02403

Zhang, Z., Liu, Y., Yuan, L., Weber, E., & van Kleunen, M. (2021). Effect of allelopathy on plant performance: a meta-analysis. *Ecology Letters*, *24*(2), 348–362. https://doi.org/10.1111/ele.13627

Supporting Information

Figure S1 Effects of *A. petiolata* treatment and tree canopy status on soil nitrate and ammonium availability

Figure S2 Effects of *A. petiolata* treatment and tree canopy status on relative chlorophyll content in *Trillium* spp. and *M. racemosum*.

Figure Legends

Figure 1 Effects of *A. petiolata* treatment and measurement period on soil inorganic nitrogen availability (a), soil phosphate availability (b), the soil nitrogen: phosphorus ratio (c), and volumetric soil moisture content (d). Tree canopy status is on the x-axis in panels a-c, while date is on the x-axis in panel d. Teal points, boxplots, and trendlines indicate measurements collected in plots where *A. petiolata* was weeded and gold points, boxplots, and trendlines indicate measurements collected in subplots where *A. petiolata* was present at ambient levels. Boxes represent the upper (75% percentile) and lower (25% percentile) quartiles, and whiskers represent 1.5 times the upper and lower quartile values. Lettering above each treatment group indicates statistically different groups where Tukey: $p<0.05$. In panel d, each point references daily volumetric soil water content averaged across the three plots used to collect gas exchange measurements, and error ribbons represent the trendline standard error.

Figure 2 Effects of *A. petiolata* treatment and tree canopy status on net photosynthesis (A_{net}, a-b), stomatal conductance (g_{sw}, c-d), and stomatal limitation of net photosynthesis (e-f). The left column shows *Trillium* spp. responses, while the right column shows *M. racemosum* responses. Tree canopy status is on the x-axis. Teal points and boxplots indicate measurements collected in plots where *A. petiolata* was weeded and gold points and boxplots indicate measurements collected in plots where *A. petiolata* abundance was not manipulated. Boxes represent the upper (75% percentile) and lower (25% percentile) quartiles, and whiskers represent 1.5 times the upper and lower quartile values. Lettering above each treatment group indicates statistically different groups where Tukey: $p<0.05$.

Figure 3 Effects of *A. petiolata* treatment and tree canopy status on the temperature-standardized maximum rate of Rubisco carboxylation (V_{cmax25}; a-b), the temperature-standardized maximum rate of electron transport for RuBP regeneration (J_{max25}; c-d), and the ratio J_{max25}:V_{cmax25} (e-f). The left column shows *Trillium* spp. responses, while the right column shows *M. racemosum* responses. Tree canopy status is on the x-axis. Teal points and boxplots indicate measurements collected in subplots where *A. petiolata* was weeded, and gold points and boxplots indicate measurements collected in subplots where *A. petiolata* abundance was not manipulated. Boxes represent the upper (75% percentile) and lower (25% percentile) quartiles, and whiskers

772 represent 1.5 times the upper and lower quartile values. Lettering above each treatment group
773 indicates statistically different groups where Tukey: $p<0.05$.

Table 1 Relative effects of *A. petiolata* ambient vs. removal treatments on soil, AM fungal, native plants, native community metrics in a long-term (2006-2025) experiment at Trillium Trail Reserve, Fox Chapel, PA.

Metric Category	Metric	*A. petiolata* effect	Evidence	Citation
Soil characteristics	Soil moisture	No change	No difference between *A. petiolata*-ambient and weeded plots	(Bialic-Murphy et al., 2021; Burke et al., 2019)
	Soil nutrient availability	No change	No difference between *A. petiolata*-ambient and weeded plots	(Bialic-Murphy et al., 2021; Burke et al., 2019)
	Soil carbon	-	Soil C is reduced in *A. petiolata*-ambient plots	(Burke et al., 2019)
AM fungal community composition and function	AM fungal spore germination	-	Reduced spore germination by *A. petiolata* allelochemicals	(Cantor et al., 2011)
	AM fungal colonization in roots	-	Lower colonization in *A. petiolata*-ambient treatment	(Mutz et al. in review; Bialic-Murphy et al., 2021)
	Soil AM fungal hyphal lengths	-	Lower fungal hyphal lengths in *A. petiolata*-ambient plots	(Cantor et al., 2011; Hale et al., 2016)
	AM fungal spore abundance in soil	No change	No change	(Burke et al., 2019)
	AM fungal diversity (richness) in soil	No change	No change	(Bialic-Murphy et al., 2021)
	AM fungal diversity (richness) in roots	No change	No change	(Mutz et al. in review)
	AM fungal community composition in soil	Change	AM fungal composition shift in mineral soil	(Bialic-Murphy et al., 2021; Burke, 2008; Burke et al., 2011, 2019)
	AM fungal community composition in native plant roots	Change	AM fungal composition shift in native plant roots	(Mutz et al. in review)
	Soil nutrient provisioning to native plants ($\delta^{15}N$)	-	Native plant $\delta^{15}N$ higher in *A. petiolata*-ambient plots	(Mutz et al. in review)
Native plant community structure	Mycorrhizal plant abundance	-	Native AM plant abundance decreases with *A. petiolata*	(Roche et al., 2021, 2023)
Native plant physiology and allocation	Stored carbon (inulin) in *Maianthemum*	-	*A. petiolata* leaf litter reduced stored carbon (inulin) in *Maianthemum*	(Hale et al., 2016)
	Soil respiration (microbial activity)	-	*A. petiolata* tissue slowed soil respiration	(Hale et al., 2011)
	Net photosynthesis in *Maianthemum*	-	*A. petiolata* decreases net photosynthesis rates	(Brouwer et al., 2015; Hale et al., 2011)
	Stomatal conductance in *Maianthemum*	-	*A. petiolata* decreases stomatal conductance	(Brouwer et al., 2015; Hale et al., 2011)
	Photosynthetic capacity (V_{cmax}, J_{max})	?	No evidence prior to this study	This study
	Temporal variation across growing season	?	No evidence prior to this study	This study

5 **Table 2** Replication statement for levels of inference used in this study

Measurement type	Scale of Inference	Scale at which the factor of interest is applied	Number of replicates at the appropriate scale
Soil nutrient availability	Plot	Plot (treatment is imposed in split-plot design)	3 plots x 6 resin strips per nutrient type per *A. petiolata* treatment per plot (12 resin strips per nutrient type per plot) = 18 replicates per nutrient type per *A. petiolata* treatment (36 total resin strips per nutrient across plots)
Soil moisture	Plot	Plot (treatment is imposed in split-plot design)	3 plots x 1 soil moisture sensor per *A. petiolata* treatment (2 soil moisture sensors per plot) = 3 replicates per *A. petiolata* treatment
Native plant photosynthetic traits	Species	7 photosynthetic traits per individual	4-20 individuals per species per *A. petiolata* treatment per plot. Total number of individuals per species: 33 *Trillium* spp. individuals, 32 *M. racemosum* individuals

6

7

Table 3 Analysis of variance results exploring the role of *A. petiolata* treatment and measurement period on soil nitrogen and phosphorus availability*

		A. petiolata treatment (A)		Canopy status (C) or day of year (D)		A×C or A×D	
	df	χ^2	*p*	χ^2	*p*	χ^2	*p*
Soil nitrogen availability	1	2.648	0.104	51.242	**<0.001**	2.438	0.118
Soil NO_3-N availability	1	2.609	0.106	63.730	**<0.001**	1.719	0.190
Soil NH_4-N availability	1	0.038	0.845	0.086	0.770	1.072	0.301
Soil phosphate availability	1	2.589	0.108	10.355	**0.001**	0.297	0.586
Soil N:P	1	3.115	*0.078*	24.827	**<0.001**	0.181	0.670
Soil moisture	1	17.778	**<0.001**	310.951	**<0.001**	0.272	0.602

*Significance determined using Type II Wald χ^2 tests (α=0.05). *P*-values less than 0.05 are in bold, while $0.05<p<0.1$ are in italic font. Soil nutrient availabilities report results using *A. petiolata* treatment, canopy status, and their interaction as fixed effects, while soil moisture reports results using *A. petiolata* treatment, day of year, and their interaction as fixed effects.

Key: df = degrees of freedom

Table 4 Analysis of variance results for the effects of *A. petiolata* treatment and measurement period on leaf gas exchange*

	A_{net}		g_{sw}		Stomatal limitation		*SPAD*	
	χ^2	*p*	χ^2	*p*	χ^2	*p*	χ^2	*p*
***Trillium* spp.**								
A. petiolata treatment (A)	3.439	*0.064*	0.123	0.726	0.101	0.751	0.061	0.805
Canopy status (C)	774.777	**<0.001**	12.969	**<0.001**	284.608	**<0.001**	77.290	**<0.001**
A×C	4.593	**0.032**	0.864	0.353	0.041	0.839	4.602	**0.032**
M. racemosum								
A. petiolata treatment (A)	5.790	**0.016**	9.280	**0.002**	7.452	**0.006**	1.486	0.223
Canopy status (C)	248.591	**<0.001**	132.846	**<0.001**	7.336	**0.007**	332.988	**<0.001**
A×C	0.301	0.583	0.199	0.656	5.204	**0.023**	2.338	0.126

*Significance determined using Type II Wald χ^2 tests (α=0.05). *P*-values less than 0.05 are in bold and 0.05<*p*<0.1 are in italics. Key: A_{net} = light-saturated net photosynthesis rate (μmol m^{-2} s^{-1}), g_{sw} = stomatal conductance (mol m^{-2} s^{-1}), SPAD = relative chlorophyll content (unitless)

Table 5 Analysis of variance results for the effects of *A. petiolata* treatment and measurement period on apparent photosynthetic capacity*

	V_{cmax25}		J_{max25}		J_{max25}:V_{cmax25}	
	χ^2	*p*	χ^2	*p*	χ^2	*p*
***Trillium* spp.**						
A. petiolata treatment (A)	2.188	0.139	5.103	**0.024**	3.764	*0.052*
Canopy status (C)	1513.276	**<0.001**	1472.096	**<0.001**	10.561	**0.001**
A×C	4.569	**0.033**	6.070	**0.014**	1.739	0.187
M. racemosum						
A. petiolata treatment (A)	<0.001	0.992	0.004	0.948	0.181	0.671
Canopy status (C)	260.475	**<0.001**	310.714	**<0.001**	0.928	0.335
A×C	0.417	0.519	0.006	0.937	2.070	0.150

*Significance determined using Type II Wald χ^2 tests (α=0.05). *P*-values less than 0.05 are in bold and values where $0.05<p<0.1$ are italicized. Key: V_{cmax25} = maximum rate of Rubisco carboxylation at 25°C (μmol m^{-2} s^{-1}), J_{max25} = maximum rate of electron transport for RuBP regeneration at 25°C (μmol m^{-2} s^{-1}), J_{max25}:V_{cmax25} = ratio of J_{max25} to V_{cmax25} (unitless)

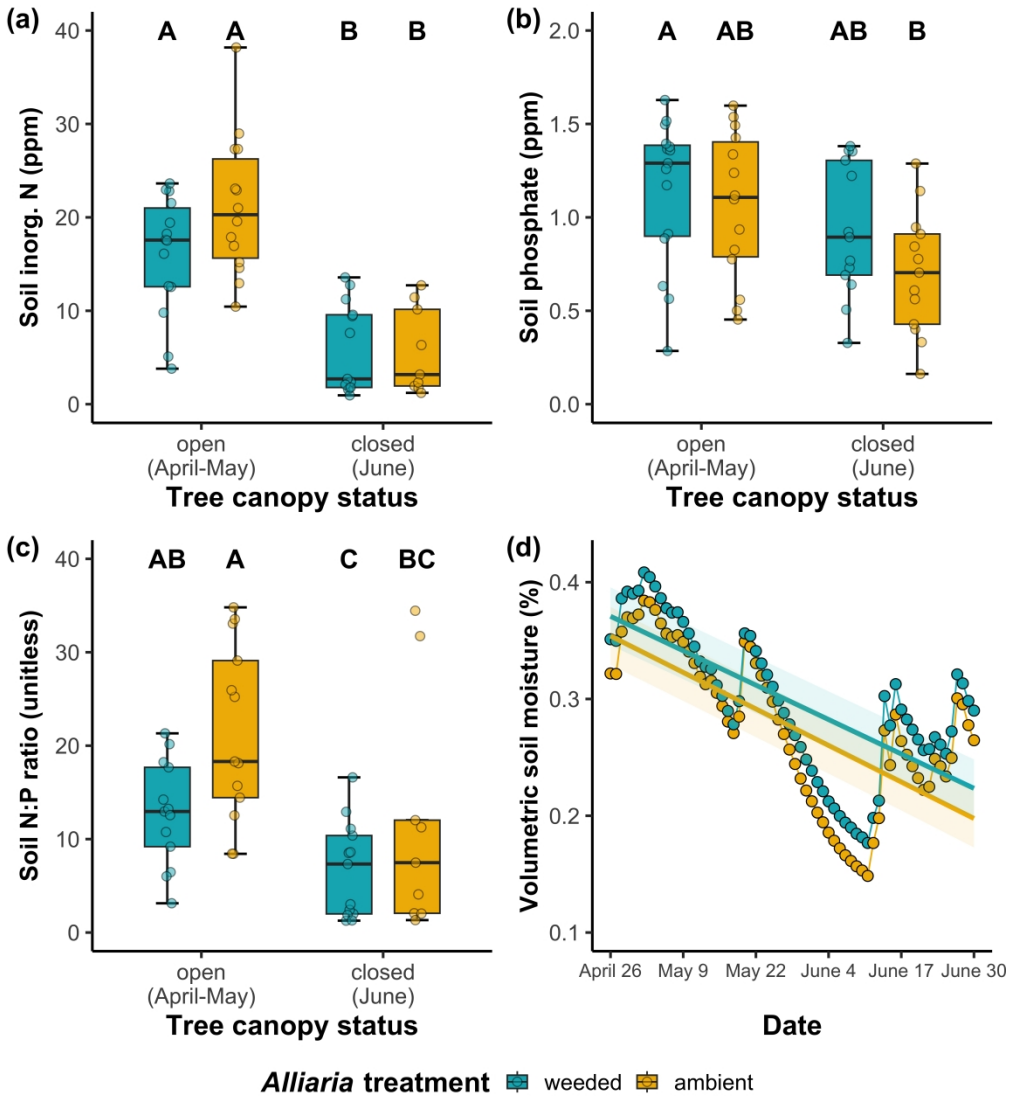

Effects of *A. petiolata* treatment and measurement period on soil inorganic nitrogen availability (a), soil phosphate availability (b), the soil nitrogen: phosphorus ratio (c), and volumetric soil moisture content (d). Tree canopy status is on the x-axis in panels a-c, while date is on the x-axis in panel d. Teal points, boxplots, and trendlines indicate measurements collected in plots where *A. petiolata* was weeded and gold points, boxplots, and trendlines indicate measurements collected in subplots where *A. petiolata* was present at ambient levels. Boxes represent the upper (75% percentile) and lower (25% percentile) quartiles, and whiskers represent 1.5 times the upper and lower quartile values. Lettering above each treatment group indicates statistically different groups where Tukey: $p<0.05$. In panel d, each point references daily volumetric soil water content averaged across the three plots used to collect gas exchange measurements, and error ribbons represent the trendline standard error.

1905x2116mm (72 x 72 DPI)

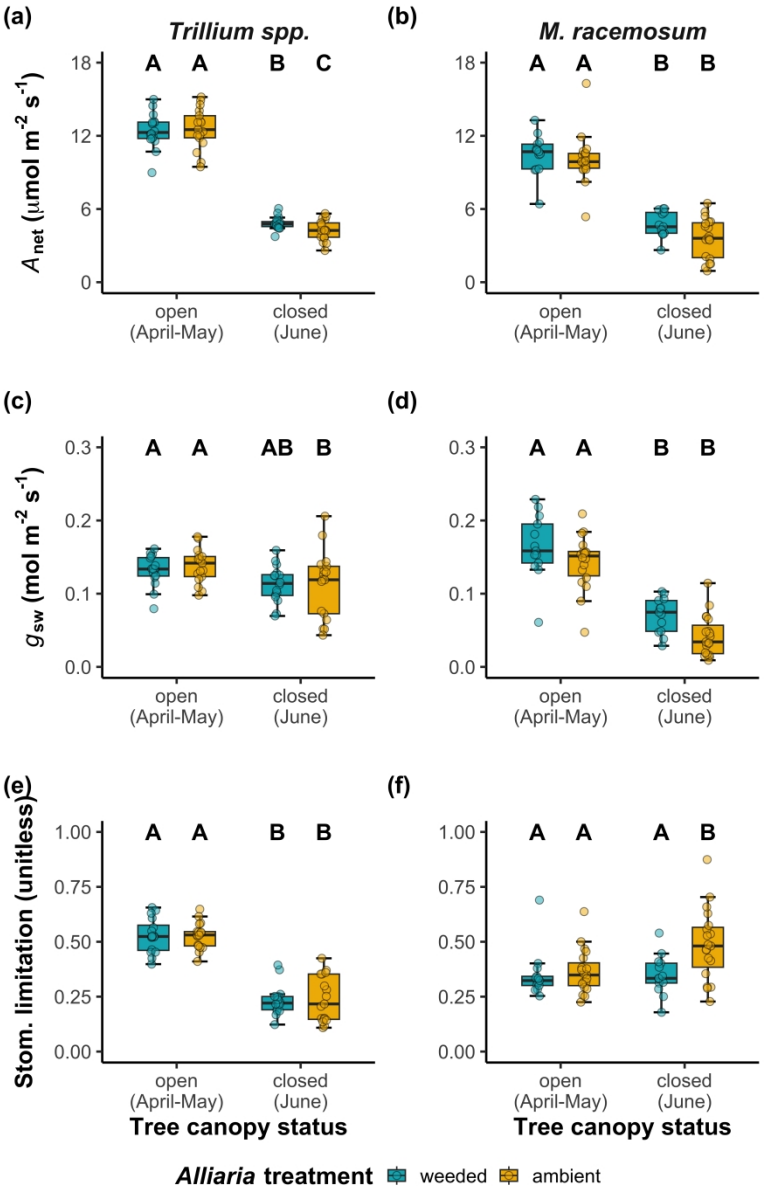

Effects of *A. petiolata* treatment and tree canopy status on net photosynthesis (A_{net}, a-b), stomatal conductance (g_{sw}, c-d), and stomatal limitation of net photosynthesis (e-f). The left column shows Trillium spp. responses, while the right column shows M. racemosum responses. Tree canopy status is on the x-axis. Teal points and boxplots indicate measurements collected in plots where A. petiolata was weeded and gold points and boxplots indicate measurements collected in plots where A. petiolata abundance was not manipulated. Boxes represent the upper (75% percentile) and lower (25% percentile) quartiles, and whiskers represent 1.5 times the upper and lower quartile values. Lettering above each treatment group indicates statistically different groups where Tukey: $p<0.05$.

1693x2645mm (72 x 72 DPI)

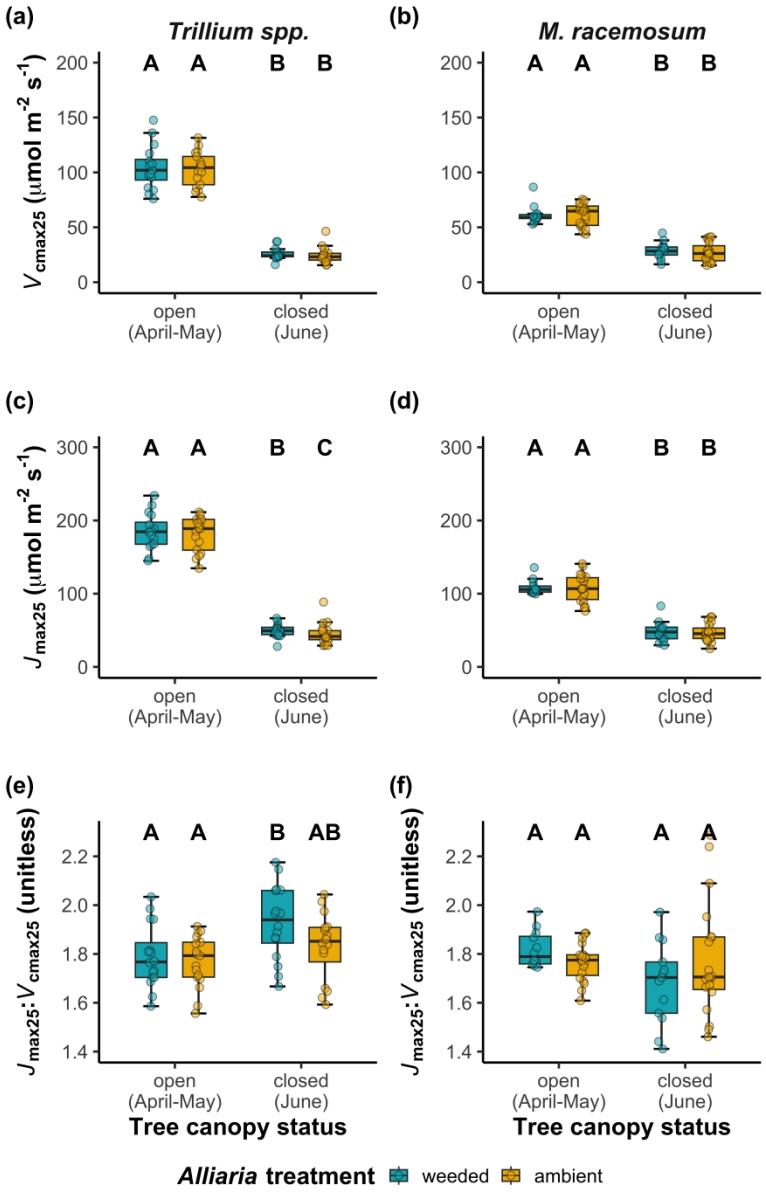

Effects of *A. petiolata* treatment and tree canopy status on the temperature-standardized maximum rate of Rubisco carboxylation (V_{cmax25}; a-b), the temperature-standardized maximum rate of electron transport for RuBP regeneration (J_{max25}; c-d), and the ratio J_{max25}:V_{cmax25} (e-f). The left column shows *Trillium* spp. responses, while the right column shows *M. racemosum* responses. Tree canopy status is on the x-axis. Teal points and boxplots indicate measurements collected in plots where *A. petiolata* was weeded and gold points and boxplots indicate measurements collected in plots where *A. petiolata* abundance was not manipulated. Boxes represent the upper (75% percentile) and lower (25% percentile) quartiles, and whiskers represent 1.5 times the upper and lower quartile values. Lettering above each treatment group indicates statistically different groups where Tukey: $p<0.05$.

1693x2645mm (72 x 72 DPI)

SUPPLEMENTAL MATERIAL for "Negative effects of allelopathic plant invasion accumulate as the growth season progresses"

Figure S1

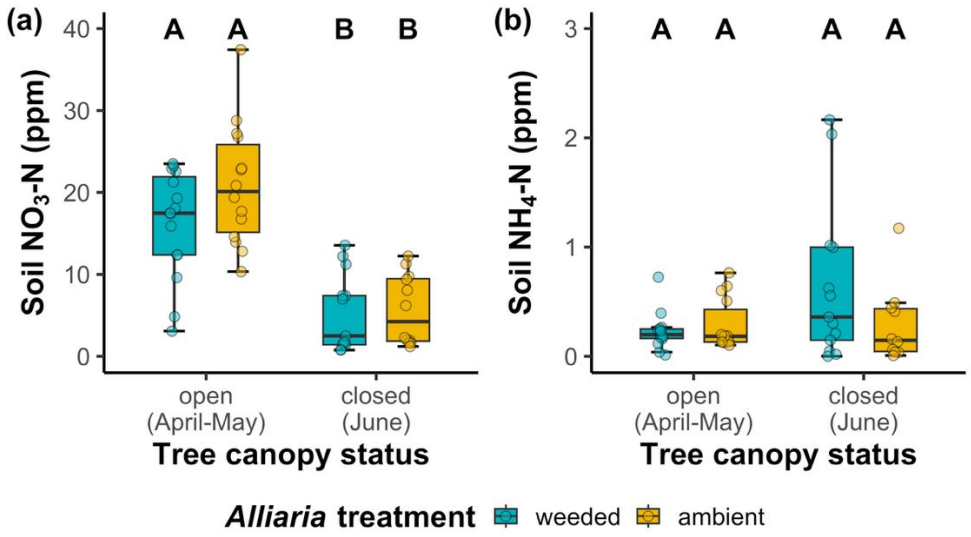

Figure S1 Effects of *A. petiolata* treatment and tree canopy status on soil nitrate availability (a) and soil ammonium availability (b). Tree canopy status is on the x-axis. Teal points and boxplots indicate measurements collected in plots where *A. petiolata* was weeded and gold points and boxplots indicate measurements collected in subplots where *A. petiolata* was present at ambient levels. Boxes represent the upper (75% percentile) and lower (25% percentile) quartiles, and whiskers represent 1.5 times the upper and lower quartile values. Lettering above each treatment group indicates statistically different groups where Tukey: $p<0.05$.

Figure S4

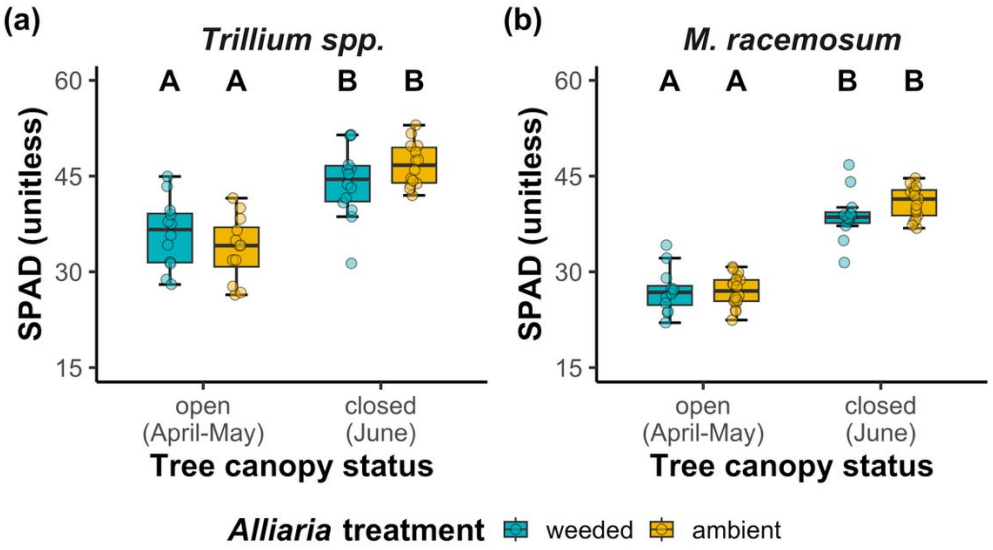

Figure S2 Effects of *A. petiolata* treatment and tree canopy status on relative chlorophyll content in *Trillium* spp. (a) and *M. racemosum* (b). Tree canopy status is on the x-axis. Teal points and boxplots indicate measurements collected in plots where *A. petiolata* was weeded and gold points and boxplots indicate measurements collected in subplots where *A. petiolata* was present at ambient levels. Boxes represent the upper (75% percentile) and lower (25% percentile) quartiles, and whiskers represent 1.5 times the upper and lower quartile values. Lettering above each treatment group indicates statistically different groups where Tukey: $p<0.05$.